Investigation of System Efficiency Improvement Through Heat Pump Application in ABC Test Loop Stage II

Byeongmin Kang[a], Gihyeon Kim [a], Jeong Ik Lee[*]
[a]*Department of Nuclear and Quantum Engineering, KAIST, 291 Daehak-ro, Yuseong-gu, Daejeon 34141, Republic of Korea*
[*]*Corresponding author: jeongiklee@kaist.ac.kr*

Keywords : Supercritical CO_2 brayton cycle, heat pump, thermodynamic analysis

1. Introduction

As a part of ongoing research on supercritical carbon dioxide ($S-CO_2$) power conversion systems, this study investigates methods to enhance cycle efficiency through heat pump integration. $S-CO_2$ systems are recognized for their high energy efficiency and compact size, leveraging the unique fluid properties near the critical point. At KAIST, the ABC (Autonomous Brayton Cycle) Test Loop Stage II has been developed to experimentally verify the performance of key components such as heat exchangers and turbomachinery [1].

To further improve the system's performance, the application of a heat pump is explored as a replacement for conventional electric heaters. While the current system relies on external heat sources, the integration of a trans-critical CO_2 heat pump can potentially maximize overall energy utilization. In this study, a mathematical model for quasi-steady-state thermodynamic analysis was developed using Python, incorporating KAIST-TMD(Turbo Machinery Design) and KAIST-HXD(Heat eXchanger Design) codes for component evaluation. This paper describes the identified design conditions for the heat pump and presents representative results, including the COP (Coefficient of Performance) of the proposed system and the impact of turbine re-design on efficiency.

2. Methods and Results

In this study, the ABC Test Loop Stage II was modeled using Python to analyze system behavior under various initial conditions. Based on the simulation results, the operational requirements for heat pump integration were identified, and the heat pump system was subsequently designed to meet these specific conditions.

2.1 ABC TEST LOOP STATE II

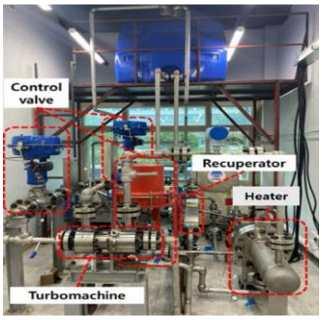

Fig. 1. An image of ABC test loop stage II with its constituent elements identified [2].

The ABC Test Loop Stage II is a simple recuperated cycle comprising a turbine, compressor, heater, precooler, and recuperator, designed to test supercritical carbon dioxide as a working fluid for a power plant's secondary system.
The system generates work by receiving external heat through a heater. This study aims to replace the conventional heater with a heat pump to reduce energy consumption, thereby facilitating the achievement of a break-even state more effectively.

2.2 KAIST – HXD

The KAIST-HXD code implements the temperature change using the 1D-FDM (Finite Difference Method) method and applies the iterative pressure drop method to calculate the fluid's temperature and pressure drop. To numerically solve the governing partial differential equations in the heat exchanger model, the 1D FDM is applied [4]. This method discretizes the spatial domain into a finite number of nodes and approximates the derivatives in the partial differential equations using algebraic expressions involving neighboring node values [5,6].

By applying the algorithm of KAIST-HXD, the changes in fluid conditions, such as temperature distribution, pressure drop, and heat transfer rate, can be accurately captured throughout the heat exchanger

2.3 KAIST-TMD

In a radial compressor, the fluid passes through the impeller, diffuser, and volute, while in a radial turbine, the fluid passes through the volute, nozzle, and rotor.

Based on the NIST-REFPROP data, the 1D-stream line method is used to track the changes in temperature, pressure, and enthalpy of the fluid. The Loss option allows for the inclusion of thermodynamic losses that occur as the fluid passes through the turbomachine [7]. These various conditions are then evaluated using the NIST REFPROP database, which helps calculate the fluid properties at the inlet and outlet, ensuring that the state of the fluid in the turbomachine is always monitored.
The design points for the turbine and compressor are summarized in Table 1 and Table 2, respectively. Subsequently, off-design performance analysis will be conducted under various operating conditions using the KAIST -TMD code.

Table 1: Turbine design conditions

Turbine type		Single stage centrifugal turbine
Turbine pressure ratio		1.11
Mass flow [kg/s]		1.5
Maximum RPM		36,000
Nozzle type		Vaneless nozzle
Inlet Condition	Pressure [MPa]	8.9
	Temperature [°C]	60
Blade Number		10
Axial Velocity [m/s]		15.5
Rotor hub diameter at exit [m]		0.00419
Clearance		0.000254

Table 2: Compressor design conditions

Compressor type		Single stage centrifugal compressor
Compressor pressure ratio		1.2
Mass flow [kg/s]		1.5
Maximum RPM		36,000
Diffuser type		Vaneless diffuser
Inlet Condition	Pressure [MPa]	7.6
	Temperature [°C]	35
Blade Number		18
Backswept Angle [°]		50
Axial Velocity [m/s]		15.5
Rotor hub diameter at exit [m]		0.0207497
Clearance		0.000254

2.4 Optimization algorithm

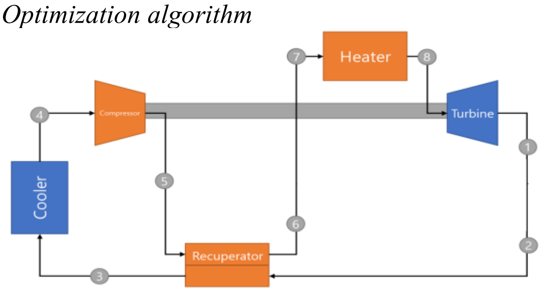

Fig. 2(a). A diagram of the ABC test loop stage II. A simulation is designed based on this simplified structure.

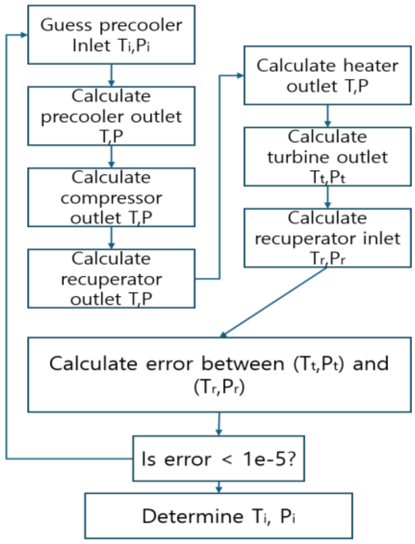

Fig. 2(b). Convergence Algorithm for initial condition

Based on the two in-house codes described at sections 2.2 and 2.3, the ABC Test Loop Stage II was implemented as a single integrated simulation program. Figure 2(a) illustrates a simplified schematic of the structure shown in Figure 1, with arrows indicating the direction of the fluid flow. For the simulation, the inlet of the cooler was established as the fixed condition for the analysis. The overall flow of the cycle proceeds as follows: In the simplified model above, the algorithm starts with condition 3 as the initially guessed state, and the fluid passes through the precooler, compressor, recuperator, heater, and turbine. This temperature and pressure of the fluid is condition 1, after passing through these components. Then, by reverse calculating the temperature and pressure changes when the fluid passes through the recuperator starting from precooler inlet, the temperature and pressure conditions of the fluid at recuperator inlet are calculated and this is condition 2. When the difference between conditions 1 and 2 is less than 10^{-5}, the two fluids are at the same conditions, and the temperature and pressure conditions of the cycle are well predicted. To obtain these results, a wide range of initial temperature and pressure conditions was established, and the bisection method was employed to iteratively narrow down the range of these initial conditions [8].

In the cycle configured as shown in Figure 2(b), the fluid flow rate is reduced from 1.5 kg/s by 0.1 kg/s increments to explore the conditions based on the fluid flow. Additionally, RPM varies from 36,000 RPM to 24,000 RPM, in steps of 3,000 RPM, to assess the impact of the turbomachine's performance on the cycle. Finally, the heater power is increased from 50 kW by increments of 10 kW up to 250 kW to analyze how the cycle efficiency changes as the heater power increases.

2.5 System without heat pump

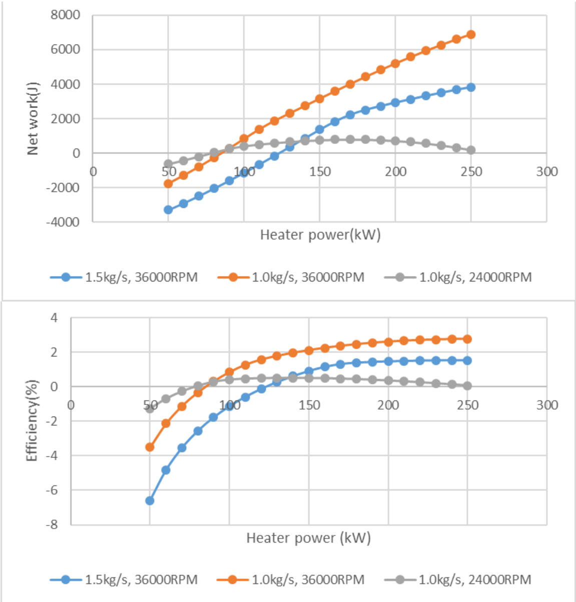

Fig 3. The net work and net efficiency of the system derived from the simulation. To optimize system cooling and maintenance, it was decided to utilize fluid conditions of 1kg/s and 24,000RPM, which require the minimum heater output.

The thermodynamic performance, including net work and thermal efficiency, was evaluated following the integration of the re-designed turbine. Unlike the original configuration, the turbine efficiency was set to 80% to ensure the system can generate positive net work, thereby validating the feasibility of the integrated cycle. The analysis demonstrated that system performance is significantly influenced by the correlation between mass flow rate and rotational speed. When the mass flow rate was reduced from 1.5 kg/s to 1 kg/s, a notable decrease in flow velocity was observed. While higher velocities at 1.5 kg/s typically enhance turbine output, they also introduce greater flow-induced losses, suggesting that a reduced flow rate can be advantageous for optimizing internal efficiency.

Furthermore, the impact of rotational speed was examined at a constant flow rate of 1 kg/s. A reduction in RPM from 36,000 to 24,000 resulted in a distinct shift in the performance curve. At the lower speed of 24,000 RPM, the compressor was unable to provide sufficient pressure rise, and since the turbine outlet pressure remained fixed, both the turbine output and the overall net work decreased accordingly.

Table 3: Conditions for components from simulation

Component	Inlet Temp. (°C)	Inlet Pres. (bar)	Outlet Temp. (°C)	Outlet Pres. (bar)
Compressor	35	84.08	40.29	99.63
Recuperator (Cold)	40.29	99.63	40.31	99.30
Heater	40.31	99.30	51.59	98.86
Turbine	51.59	98.86	41.95	85.10
Recuperator (Hot)	41.95	85.10	41.91	84.50
Precooler	41.91	84.50	35	84.08

Despite these variations, the study successfully identified specific operating points tailored to different research priorities. For instances requiring maximum turbine output, 1.5 kg/s at 36,000 RPM proved optimal, whereas 1 kg/s at 36,000 RPM yielded the highest net work. However, as the primary objective of this study is to achieve a self-sufficient break-even cycle while minimizing external heat input, the condition of 1 kg/s and 24,000 RPM was selected as the final design basis. This operating point minimizes the required heater power, which not only facilitates more efficient cooling system integration but also simplifies the long-term maintenance of the ABC Test Loop Stage II. The off-design turbine efficiency identified through the KAIST-TMD code under these flow rate and RPM conditions was 75.81%, which shows no significant discrepancy compared to the initial turbine efficiency setting of 80%. It is expected that the target efficiency of 80% can be achieved and experimentally validated in the future by modifying the turbine design point or identifying further improvements.

2.6 Heat pump application

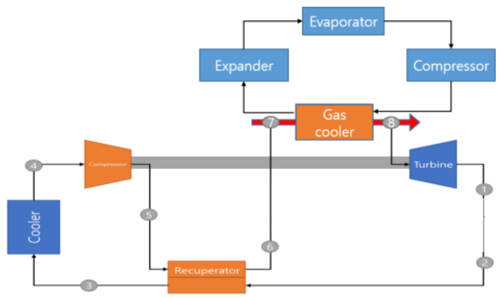

Fig. 4. A schematic diagram of the system where the conventional heater is replaced by a heat pump. The heat pump is designed to deliver 80 kW of thermal power to the ABC Test Loop Stage II, matching the capacity of the original electric heater.

In this study, a trans-critical CO_2 heat pump system was designed to replace the conventional electric heater in the ABC Test Loop Stage II. Fig. 4 illustrates the schematic diagram of the heat pump system designed for this application. Each constituent component of the heat pump was integrated into the Python-based simulation environment, utilizing the established KAIST-HXD and KAIST-TMD codes.

This system was selected because it effectively meets the required temperature and pressure lift while utilizing the same working fluid as the main cycle [9], thereby minimizing structural modifications and enhancing maintenance convenience. The system is configured to absorb heat from an external ambient source and elevate it to a high-temperature, high-pressure state through a compression process to meet the thermal requirements of the power cycle.

The heat pump's compressor elevates saturated CO_2 to a high-pressure state with an isentropic efficiency of 75%, a value adopted from established turbomachinery design specifications for $S-CO_2$ systems. To ensure operational safety within the ABC Test Loop Stage II, the discharge pressure was limited to 12 MPa, which corresponds to the system's maximum allowable pressure. To maximize the COP an expander was integrated to recover mechanical work from the high-pressure fluid exiting the gas cooler. This recovered work partially offsets the compressor's power consumption. Based on on-design calculations using the KAIST-TMD code, the expander operates at 17,000 RPM with an efficiency of 85%, producing approximately 15 kW of mechanical work.

The gas cooler, designed as a Printed Circuit Heat Exchanger (PCHE), utilizes the same channel geometry and flow path length as the recuperator modeled via KAIST-HXD. In the gas cooler, the heat pump fluid is cooled by rejecting heat while maintaining a supercritical state without a separate condensation process, thereby serving to supply heat to the system. Analysis confirmed that with a gas cooler inlet temperature of 62.5°C, the system can heat the supercritical CO_2 from 40.31°C to 51.59°C. This allows the system to supply a thermal load of 80 kW, which is equivalent to the capacity of the conventional electric heater.

To evaluate the thermodynamic performance, a simulation was conducted under an inlet fluid temperature of 10°C and ambient condition, consistent with the conditions used in the previous studies [10]. The results demonstrated that the power required to compress the saturated CO_2 to 12 MPa was 49.18 kW.

By utilizing the 15 kW of power generated by the expander to reduce the net electrical input, the final COP was determined to be 2.34. The results were derived through on-design calculations using the existing algorithm and were conducted with reference to established research data [11]. The resulting values are close to the COP of 2.5 typically observed in conventional trans-critical heat pump studies [12]. This result demonstrates that the trans-critical CO_2 heat pump can achieve the required heating duty while significantly reducing external energy consumption compared to direct electric heating.

3. Conclusions

This study demonstrates that the integration of a heat pump into the ABC Test Loop can contribute to significant performance enhancements compared to the conventional system. For practical implementation, it is essential to design a heat pump that meets specific temperature and pressure requirements, supported by turbomachinery and facilities capable of maintaining target efficiency. Furthermore, to maximize the advantages of the heat-pump-integrated system, future research should explore methodologies for coupling this system with Energy Storage Systems.

ACKNOWLEDGEMENT

This work was supported by the National Research Foundation of Korea(NRF) grant funded by the Korea government(MSIT) (No. RS-2025-25454059).

REFERENCES

[1]Dostal, V., Hejzlar, P., & Driscoll, M. J. (2004). Supercritical CO_2 Cycle for Next Generation Nuclear Reactors:

[3] Baek, J. M., & Lee, J. I. Supercritical CO2 Brayton Cycle Research at KAIST: Achieving Breakeven Conditions in the Autonomous Brayton Cycle (ABC) Test Loop.

[2] Baek, J. Y., Lee, J. J., & Lee, J. I. (2022). System modeling of KAIST S-CO2 ABC test loop. *Trans. Korean Nucl. Soc. Spring Meet*.

[4] Son, I. W., & Leea, J. I. (2021). The concept design of the nuclear-renewable hybrid system: Component designs for different Nuclear-Renewable heat ratio.

[5] Baik, S., Kim, S. G., Lee, J., & Lee, J. I. (2017). Study on CO2–water printed circuit heat exchanger performance operating under various CO_2 phases for S-CO_2 power cycle application. *Applied Thermal Engineering*, *113*, 1536-1546.

[6] J. Li, Y. Hu, X. Zhang, W. Xu, M. Cai and G. Jia, "Energy Efficiency Analysis of the Pre-cooling Air Compressor System," *2023 9th International Conference on Fluid Power and Mechatronics (FPM)*, Lanzhou, China, 2023, pp. 01-07, doi: 10.1109/FPM57590.2023.10565458.

[7] Lee, S., & Lee, J. I. (2023). Validation of KAIST-TMD with recent supercritical CO2 Turbine-Alternator-Compressor test data.

[8] W. Cheney and D. Kincaid, "Numerical Mathematics and Computing". 6th edition, Thomson Brooks/Cole, 2008.

[9] Ye, Z., Wang, Y., Song, Y., Yin, X., & Cao, F. (2020). Optimal discharge pressure in transcritical CO2 heat pump water heater with internal heat exchanger based on pinch point analysis. *International Journal of Refrigeration*, *118*, 12-20.

[10] Austin, B. T., & Sumathy, K. (2011). Transcritical carbon dioxide heat pump systems: A review. *Renewable and Sustainable Energy Reviews*, *15*(8), 4013-4029.

[11] Fuller, R., Hemrle, J., & Kaufmann, L. (2013, June). Turbomachinery for a Supercritical CO2 Electro-Thermal Energy Storage System. In *Turbo Expo: Power for Land, Sea, and Air* (Vol. 55294, p. V008T34A011). American Society of Mechanical Engineers.

[12] MAN Energy Solutions. (n.d.). High-temperature heat pump using CO_2 as refrigerant (HPU series) [Brochure]. Retrieved June 18, 2025, from https://www.man-es.com/docs/default-source/document-sync-archive/man-heat-pump-hpu-eng.pdf?sfvrsn=e83c2883_6